2014 22nd International Conference on Pattern Recognition

Graph Characterization using Wave Kernel Trace

Furqan Aziz, Richard C. Wilson, Edwin R. Hancock
Department of Computer Science
University of York
York, UK, YO105GH
Email: {furqan,wilson,erh}@cs.york.ac.uk

***Abstract*—Graph based methods have been successfully used in computer vision for classification and matching. This is due to the fact that shapes can be conveniently represented using graph structures. In this paper we explore the use of a spectral invariant which is based on the wave kernel trace to characterize graphs. The wave kernel is the solution of wave equation defined using the Edge-based Laplacian of a graph. The advantage of using the edge-based Laplacian over its vertex-based counterpart is that it can be used to translate equations from continuous analysis to the discrete graph theoretic domain, that have no meanings if defined using vertex-based Laplacian. To illustrate the utility of the proposed method we apply it to graphs extracted from both three-dimensional shapes and images.**

I. Introduction

Graph structures have proved important representative tools in many areas including computer vision, machine learning and pattern recognition. This is due to the fact that graphs can be considered as the most generic data structure to represent objects. However one of the limitations with graphs are that they have no ordering relations, and therefore they cannot be easily converted in to pattern vectors. As a result methods from statistical learning cannot be directly applied to graph. In order to overcome this problem, many approaches have been proposed to convert graphs to feature vectors in a permutation-invariant manner. Most of these approaches either use spectral methods (eigenvalues and eigevectors of the matrix representation of the graph) or the frequencies with which a particular substructure appears in the graph. Methods falling into the former category includes the use of the truncated Laplacian and symmetric polynomials [1]. Those falling into the latter category include random walks on graphs [2] and Ihara coefficients [3].

An alternative approach to construct feature vectors from graph is to use the solution of partial differential equation defined using the vertex-based Laplacian of the graph. The vertex-based Laplacian is a discrete analogue of the Laplacian in analysis and can be used to translate physical equation from the continuous domain to the discrete graph theoretic domain. To this end Xiao et al [4] have used the heat kernel to embed the nodes of a graph in a Euclidean space. The heat kernel is the solution of the heat equation and is a compact representation of the path-length distribution on a graph. They have used the resulting distribution of the embedded nodes to construct a feature vector for characterizing graph. In related works Xiao et al [5] have used the trace of the heat kernel to characterize graphs. Similarly Sun et al [6] have used the trace of the heat kernel to define the so called heat kernel signature (HKS) for characterizing points on the surface of a three dimensional shape. Castellani et al [7] have used HKS to define a Global Heat Kernel Signature (GHKS) and have used this for brain classification. Aubry et al [8] have proposed the Wave Kernel Signature (WKS) which is based on the solution of Schrödinger equation. Recently Suau et al [9] have analyzed the Schrödinger Operator in the Context of Graph Characterization.

However, the discrete Laplacian defined over the vertices of a graph does not link most of the results from the analysis of continuous Laplacians to a direct graph theoretic analogue. As a result, although the heat equation can be mapped from the continuous domain onto a graph, the wave equation cannot be mapped in this way. In an attempt to overcome this problem, Friedman and Tillich [10] have studied a new type of wave equation on graphs that involves an analogue of the wave equation in analysis. While the method leads to the definition of both a divergence operator and a Laplacian, it is not exhaustive in the sense that the edge-based eigenfunctions are not fully specified. We have recently explored the methods for computing eigenfunctions of edge-based Laplacian [11]. This reveals a connection between the eigenfunctions of the edge-based Laplacian and both the classical random walk and the backtrackless random walk on a graph.

Although the discrete Laplacian has been extensively used in the literature, little work has been done on graph characterization using the solutions of partial differential equations defined using the edge-based Laplacian. Initial work by ElGhawalby and Hancock [12] has revealed some of the potential uses of the edge-based Laplacian. To this end we have recently explored the use of the wave equation defined using the edge-based Laplacian for graph characterization. We have solved wave equation on graph [13] and used its solution to characterize graphs extracted from images of 3D shapes [14]. In related work we have used the solution of edge-based heat equation to define signature to characterize 3D shapes [15]. In this paper our goal is to explore the use of the wave kernel trace for characterizing graphs extracted from both images and three-dimensional shapes. We commence by introducing the eigenpairs of the edge-based Laplacian of a graph. Next we define signature for graph, which is based on the wave kernel trace. Finally, we apply the proposed method to graphs extracted from images and three-dimensional shapes.

II. Graphs

We commence by giving some definitions and notation. A *graph* $G = (V, E)$ consists of a finite nonempty set V of *vertices* and a finite set E of unordered pairs of vertices, called *edges*. A *directed graph* or *digraph* $D = (V_D, E_D)$ consists of a finite nonempty set V_D of vertices and a finite set E_D

1051-4651/14 $31.00 © 2014 IEEE
DOI 10.1109/ICPR.2014.656

of ordered pairs of vertices, called *arcs*. So a digraph is a graph with an orientation on each edge. A digraph D is called *symmetric* if whenever (u, v) is an arc of D, (v, u) is also an arc of D. There is a one-to-one correspondence between the set of symmetric digraphs and the set of graphs, given by identifying an edge of the graph with an arc and its inverse arc on the digraph on the same vertices. We denote by $D(G)$ the symmetric digraph associated with the graph G.

The *line graph* $L(G) = (V_L, E_L)$ is constructed by replacing each arc of $D(G)$ by a vertex. These vertices are connected if the head of one arc meets the tail of another. Therefore

$$V_L = \{(u, v) \in D(G)\}$$

$$E_L = \{((u, v), (v, w)) : (u, v) \in D(G), (v, w) \in D(G)\}$$

The *oriented line graph* $OL(G) = (V_O; E_O)$ is constructed in the same way as the $L(G)$ except that reverse pairs of arcs are not connected, i.e. $((u, v), (v, u))$ is not an edge. The vertex and edge sets of $OL(G)$ are therefore

$$V_O = \{(u, v) \in D(G)\}$$

$$E_O = \{((u, v), (v, w)) : (v, w)), (u, v) \in D(G), (v, w) \in D(G), u \neq w\}$$

Figure 1(a) shows a simple graph, 1(b) its digraph, 1(c) the corresponding oriented line graph and 1(d) the corresponding line graph.

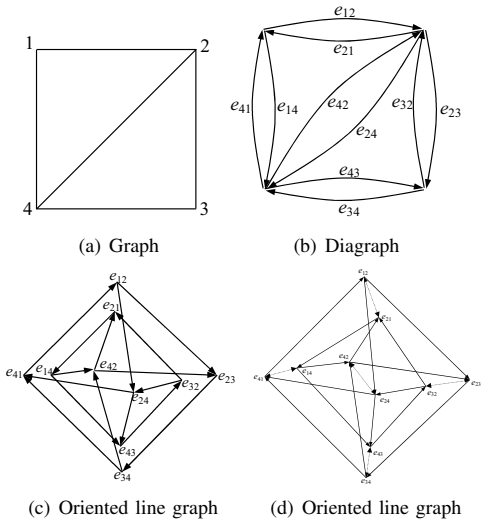

(a) Graph (b) Diagraph

(c) Oriented line graph (d) Oriented line graph

Fig. 1. Graph, its digraph, and its oriented line graph

It is interesting to note that a random walk on the vertices of a line graph corresponds to a random walk on the edges of the original graph, while a random walk on the vertices of the oriented line graph corresponds to a backtrackless walk on the edges of the original graph.

III. Edge-based Eigensystem

In this section we review the eigenvalues and eigenfunctions of the edge-based Laplacian[16] [11]. Let $G = (V, E)$ be a graph with a boundary ∂G. Let $\mathcal{G}$ be the geometric realization of G. The geometric realization is the metric space consisting of vertices V with a closed interval of length l_e associated with each edge $e \in E$. We associate an edge variable x_e with each edge that represents the standard coordinate on the edge with $x_e(u) = 0$ and $x_e(v) = 1$. For our work, it will suffice to assume that the graph is finite with empty boundary (i.e., $\partial G = 0$) and $l_e = 1$.

A. Vertex Supported Edge-based Eigenfunctions

The vertex-supported eigenpairs of the edge-based Laplacian can be expressed in terms of the eigenpairs of the normalized adjacency matrix of the graph. Let A be the adjacency matrix of the graph G, and $\tilde{A}$ be the row normalized adjacency matrix. i.e., the $(i, j)th$ entry of $\tilde{A}$ is given as $\tilde{A}(i, j) = A(i, j)/\sum_{(k,j)\in E} A(k, j)$. Let $(\phi(v), \lambda)$ be an eigenvector-eigenvalue pair for this matrix. Note that $\phi(.)$ is defined on vertices and may be extended along each edge to an edge-based eigenfunction. Let ω^2 and $\phi(e, x_e)$ denote the edge-based eigenvalue and eigenfunction. Then the vertex-supported eigenpairs of the edge-based Laplacian are given as follows:

1) For each $(\phi(v), \lambda)$ with $\lambda \neq \pm 1$, we have a pair of eigenvalues ω^2 with $\omega = \cos^{-1}\lambda$ and $\omega = 2\pi - \cos^{-1}\lambda$. Since there are multiple solutions to $\omega = \cos^{-1}\lambda$, we obtain an infinite sequence of eigenfunctions; if $\omega_0 \in [0, \pi]$ is the principal solution, the eigenvalues are $\omega = \omega_0 + 2\pi n$ and $\omega = 2\pi - \omega_0 + 2\pi n, n \geq 0$. The eigenfunctions are $\phi(e, x_e) = C(e)\cos(B(e) + \omega x_e)$ where
$$C(e)^2 = \frac{\phi(v)^2 + \phi(u)^2 - 2\phi(v)\phi(u)\cos(\omega)}{\sin^2(\omega)}$$
$$\tan(B(e)) = \frac{\phi(v)\cos(\omega) - \phi(u)}{\phi(v)\sin(\omega)}$$
There are two solutions here, $\{C, B_0\}$ or $\{-C, B_0 + \pi\}$ but both give the same eigenfunction. The sign of $C(e)$ must be chosen correctly to match the phase.
2) $\lambda = 1$ is always an eigenvalue of $\tilde{A}$. We obtain a principle frequency $\omega = 0$, and therefore since $\phi(e, x_e) = C\cos(2n\pi x_e)$ and so $\phi(v) = \phi(u) = C$, which is constant on the vertices.
3) $\lambda = -1$ is an eigenvalue of $\tilde{A}$, if the graph is bipartite. We obtain a principle frequency $\omega = \pi$, and therefore since $\phi(e, x_e) = C\cos(\pi x_e + 2n\pi x_e)$ and so $\phi(v) = C$ and $\phi(u) = -C$, which means the eigenfunction is constant with an alternating sign on both sides of bipartition.

B. Edge-interior Eigenfunctions

The edge-interior eigenfunctions are those eigenfunctions which are zero on vertices and therefore must have a principle frequency of $\omega \in \{\pi, 2\pi\}$. These eigenfunctions can be determined from the eigenvectors of the adjacency matrix of the oriented line graph.

1) The eigenvector corresponding to eigenvalue $\lambda = 1$ of the oriented line graph provides a solution in the case $\omega = 2\pi$. In this case we obtain $|E| - |V| + 1$ linearly independent solutions.
2) Similarly the eigenvector corresponding to eigenvalue $\lambda = -1$ of the oriented line graph provides a solution in the case $\omega = \pi$. If the graph is bipartite, then we obtain $|E| - |V| + 1$ linearly independent solutions. If the graph is non-bipartite, then we obtain $|E| - |V|$ linearly independent solutions.

This comprises all the principal eigenpairs which are only supported on the edges.

IV. Wave Kernel Trace

In this paper we explore the use of an invariant which is based on the wave equation defined using the edge-based Laplacian. The wave equation on the graph is defined as

$$\frac{\partial^2 u}{\partial t^2}(\mathcal{X}, t) = \Delta_E u(\mathcal{X}, t)$$

The solution of the wave equation is given as [16]

$$u(x,t) = \sum_i f_i \left(a_i cos(\omega_i t) + \frac{b_i}{\omega_i t} sin(\omega_i t) \right)$$

where a_i and b_i depends on the initial condition and ω_i^2 are the eigenvalues of the edge-based Laplacian. In a recent work, we have solved the wave equaiton on a graph, where the initial condition is a Gaussian wave packte on a particular edge of the graph[13].

An interesting spectral invariant studied in the analysis literature is the wave kernel trace (WKT), which is defined as

$$W(t) = \text{Trace}\left(\cos t\sqrt{\Delta_E}\right)$$

where Δ_E is the edge-based Laplacian. It can be simplified as

$$W(t) = \sum_j \left(\cos t\omega_j\right)$$

with ω_j^2 running through all the edge-base Laplacian eigenvalues. This is an infinite sum, and to understand this sum, Friedman et al [16] have studied the following spectral invariant

$$\tilde{W}(t) = \sum_j \left(e^{it\omega_j}\right)$$

which is a complex analytic function. We call this spectral invariant as WKTC. The WKT is just the real part of WKTC. We know that we have $\alpha_1, \alpha_2, ..., \alpha_{|E|}$, such that the edge-based eigenvalues are those squares of $\omega_i = \alpha_i + 2\pi n$ for $n \geq 0$. Then we have

$$\tilde{W}(t) = \frac{1 - e^{i2\pi t}}{4\sin^2(\pi t)} \sum_{j=1}^{2|E|} e^{it\alpha_j}$$

In this paper, we use the $\tilde{W}(t)$ to characterize a graph. We construct a feature vector by sampling $\tilde{W}(t)$ for different values of t. Since $\tilde{W}(t)$ has pole when t is integer, We construct a feature vector by setting $t = n + \frac{1}{2}$, for $n > 0$. The solution in this case becomes

$$\tilde{W}\left(n + \frac{1}{2}\right) = -\frac{1}{2}\left(|E| - |V|\right) + i\left(\sum_{j=2}^{|V|} sin\left((n + 1/2)\alpha_j\right) + \left(|E| - |V|\right)(-1)^n\right)$$

Since the real part is the same for all values of n, we therefore use the feature vector WTS, defined as

$$WTS(G) = \left[re(\tilde{W}(\frac{1}{2})), im(\tilde{W}(\frac{1}{2})), im(\tilde{W}(\frac{3}{2})), ..., im(\tilde{W}(k - \frac{3}{2}))\right]$$

of length k to characterize a graph G.

To compare the performance of the proposed signature, we compare it with a related signature extracted from the traditional Laplacian. i.e., the heat kernel trace. The heat kernel trace is the solution of the heat equation and is defined as

$$H(t) = \sum_{i=1}^{|V|} \exp\left(-\lambda_i t\right)$$

where $\lambda_1, \lambda_2, ..., \lambda_{|V|}$ are the eigenvalues of the vertex-based Laplacian. To define a signature using the heat kernel trace (called HTS), we sample the values of $H(t)$ at different time intervals. In [5] Xiao et al have shown that the HKT can be used to characterize the structure of a graph. Despite its success and elegant physical representation, one of the disadvantages of the HKT is that it is characterized by low pass frequencies. The larger the t, the more high frequencies are suppressed. This reduces the discriminative power of the HKT for larger values of t.

V. Experiments

In this section we experiment with the proposed method on graphs extracted from 3D shapes and graphs extracted from the images of 3D shapes. We commence by experimenting with the proposed method on graphs extracted from the COIL dataset [17]. The COIL dataset contains the images of 3D objects from 72 equally spaced views under controlled lighting views. To establish graphs on these images we use the Harris corner detector [18] to find feature points. These feature points are treated as the nodes of the graph.

We establish three different types of graphs over the feature points extracted from these images. i.e., Delaunay triangulations (DT) [19], Gabriel graphs (GG) [20], and relative neighbourhood graphs (RNG) [21]. A Delaunay triangulation for a set P of points in a Euclidean space is a triangulation, DT(P), such that no point in P is inside the circumcircle of any triangle in DT(P). The Gabriel graph for a set of n points is a subset of Delaunay triangulation, which connects two data points v_i and v_j for which there is no other point v_k inside the open ball whose diameter is the edge (v_i, v_j). Like the Gabriel graph, the relative neighbourhood graph is also a subset of Delaunay triangulation. In this case a lune is constructed on each Delaunay edge. The circles enclosing the lune have their centres at the end-points of the Delaunay edge; each circle has a radius equal to the length of the edge. If the lune contains

another node then its defining edge is pruned from the relative neighbourhood graph. The purpose of experiments on GG and RNG is to study the performance of the proposed method under structural modifications. Figure 2(b), Figure 2(c), and Figure 2(d) show the DT, GG and RNG of the corresponding COIL object of Figure 2(a) respectively.

(a) COIL Objects [17]

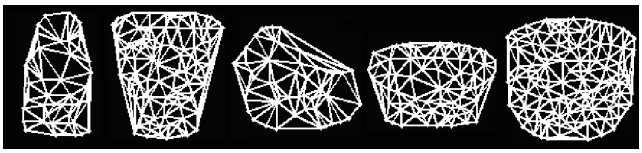

(b) Delaunay triangulations [19]

(c) Gabriel graphs [20]

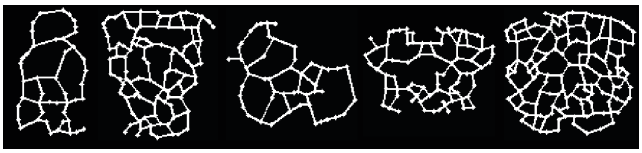

(d) Relative neighbourhood graphs [21]

Fig. 2. COIL objects and their extracted graphs

We commence by experimenting WTS on Delaunay triangulation. For this purpose we select five different objects from the dataset with all their 72 views. We have computed the WTS for each graph. To visualize the results we have performed principal component analysis (PCA) on the resulting feature vectors. PCA is mathematically defined [22] as an orthogonal linear transformation that transforms the data to a new coordinate system such that the greatest variance by any projection of the data comes to lie on the first coordinate (called the first principal component), the second greatest variance on the second coordinate, and so on. Figure 4(a) shows the visualization results of the proposed method. To compare the results, we have also computed the HKT for the same graphs. Figure 4(b) shows the visualization results for HKT.

To measure the classification accuracy and compare the performance of the proposed method, we have applied k-fold cross validation on the feature vectors computed from Delaunay triangulations for WKT, HKT, and the truncated Laplacian (TL) with $k = 9$. In a 9-fold cross validation experiment, all the 72 views of each class are partitioned into 9 subsamples each with size 8. Of the 9 subsamples, one sample is treated as validation set while the remaining 8 are treated as training data. The process is then repeated 9 times with each of the 9 subsamples used exactly once as the validation data. Table I shows the accuracy results for WKT with 4 and

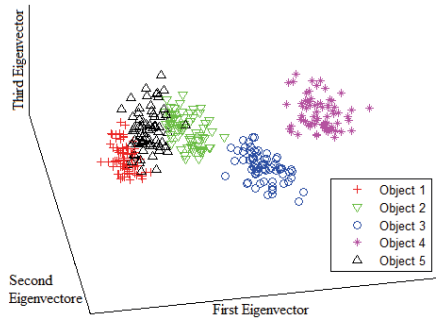

(a) WKT

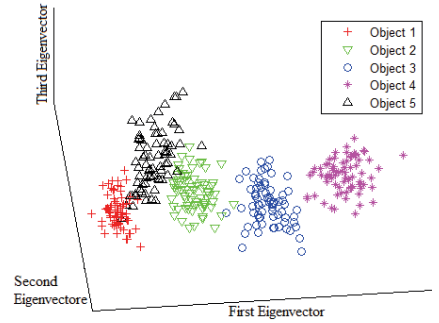

(b) HKT

Fig. 3. PCA embedding of feature vectors for DT

5 different classes and compares it with both HKT and TL. Resulsts show that WKT performs better than the alternative methods on DT.

TABLE I. EXPERIMENTAL RESULTS ON DELAUNAY

Method	4 classes	5 classes
Wave Kernel Trace	98.95%	93.05%
Heat Kernel trace	98.26%	91.94%
Truncated Laplacian	96.18%	83.89%

In our next experiment, we have compared the performance of WKT with HKT on GG and RNG. We have measured the performance using 9-fold cross validation on feature vectors of four different classes. For GG we achieved the same performance for both WTS and HTS as with DT. For RNG, we achieved the same performance as with the DT, however the performance of HKT was decreased to 97.91%. Figure 4 compares the clustering results of feature vectors computed from RNG.

We now show the stability of both HKT and WKT for different values of t. As explained earlier, one of the disadvantages of HKT is that it is characterized by low pass frequencies. The larger the value of t, the more high frequencies are suppressed. In Figure 5 we have plotted the values of HTS and WTS for each view of five different classes. Figure 5(a) and Figure 5(b) shows the values of WKT for $t = 0.5$ and $t = 1.5$, while Figure 5(c) and Figure 5(d) show the values of HKT for $t = 0.5$ and $t = 1.5$. It is clear from the figures that as the value of t increases, the discriminative power of HKT decreases. This is due to the fact that the HKT is a collection of low-pass filters, parameterized over the time t. For large value of t, high frequencies are suppressed. The WKT, on the

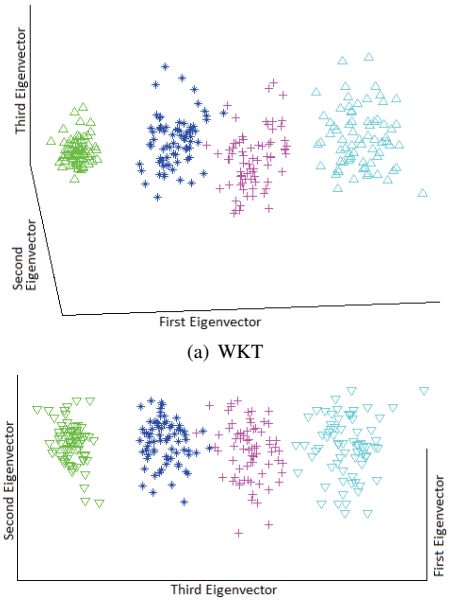

(a) WKT

(b) HKT

Fig. 4. PCA embedding of feature vectors for RNG

other hand, is parameterized over frequencies.

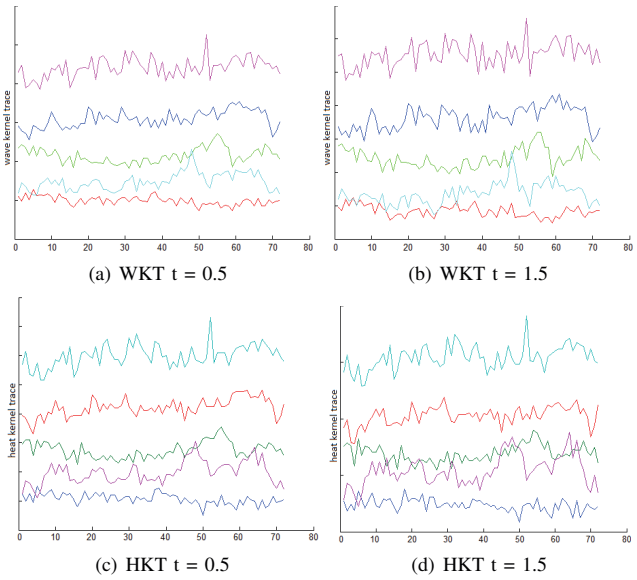

(a) WKT t = 0.5 (b) WKT t = 1.5

(c) HKT t = 0.5 (d) HKT t = 1.5

Fig. 5. HKT and WKT for different values of t

We now evaluate the performance of the proposed wave kernel feature vector on the graphs extracted from 3D shapes. For this purpose we use topological graphs, called *reeb graphs* [23], extracted from SHREC dataset. SHREC dataset contains different 3D classes, each with 20 different deformations. Figure 6 shows an example of a reeb graph, which is extracted from the shape of a horse.

To commence we have selected reeb graphs of 3 different classes with all 20 deformations. Next we have computed the

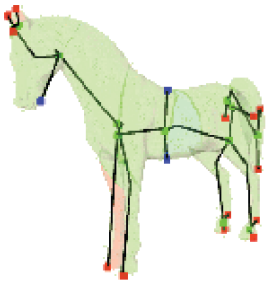

Fig. 6. An example of a reeb graph extracted from a 3D-shape of a horse

WKT, HKT, and truncated Laplacian. To visualize the results we have applied PCA to the resulting wave kernel feature vectors. Figure 7(a) shows the clustering result of the proposed method for 3 different classes, while Figure 7(b) and Figure 7(c) show similar results for HKT and TL respectively.

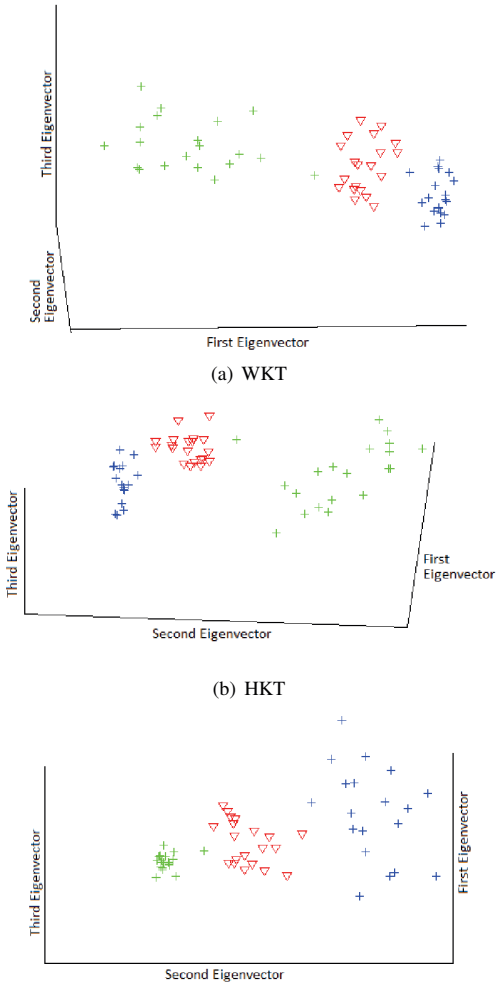

(a) WKT

(b) HKT

(c) TL

Fig. 7. PCA embedding of feature vectors for reeb graphs

We have performed a similar experiment with 4 different

classes. The clustering results are shown in Figure 8. Figure 8(a) shows the clustering result of WKT, while Figure 8(b) and Figure 8(c) show clustering results for HKT and TL respectively. Results show that WKT provides better separation between objects of different classes as compared to HKT and TL.

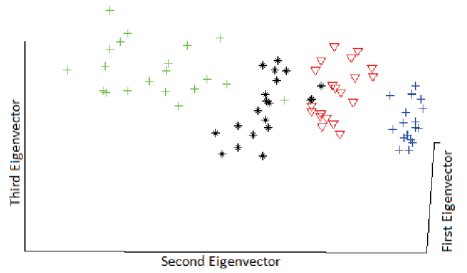

(a) WKT

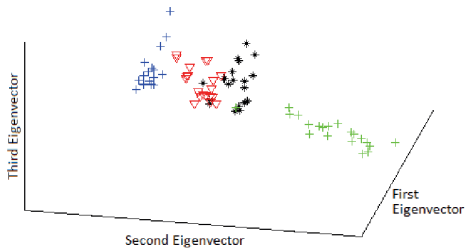

(b) HKT

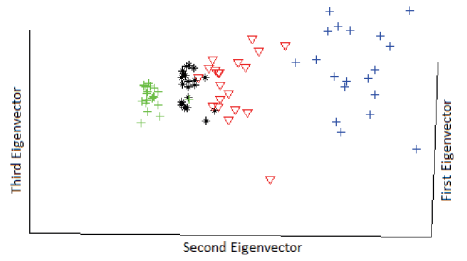

(c) TL

Fig. 8. PCA embedding of feature vectors for reeb graphs

To measure the classification accuracy of the proposed method and compare it with alternative methods, we have applied 10-fold cross validation on the feature vectors for all the three method. Table II shows the accuracy of each method. Results suggest that the WKT performs better than the alternative methods.

TABLE II. EXPERIMENTAL RESULTS ON REEB GRAPHS

Method	3 classes	4 classes
Wave Kernel Trace	98.33%	97.5%
Heat Kernel trace	98.33%	93.75%
Truncated Laplacian	96.66%	93.75%

VI. CONCLUSION

We have explored the use of the wave kernel trace for characterizing graphs which are extracted from images and 3D shapes. The wave kernel trace is the solution of wave equation defined using the edge-based Laplacian. Experimental results show that the wave kernel trace defined using the edge-based Laplacian can characterize graphs with higher accuracy compared to the heat kernel trace defined using the vertex-based Laplacian. In future, we would like to use the solutions of alternative partial differential equations defined on graphs and computed using the edge-based Laplacian.

REFERENCES

[1] R. C. Wilson, E. R. Hancock, and B. Luo, "Pattern vectors from algebraic graph theory," *IEEE Transactions on Pattern Analysis and Machine Intelligence*, pp. 1112–1124, 2005.

[2] T. Gartner, P. Flach, and S. Wrobel, "On graph kernels: Hardness results and efficient alternatives," *16 Annual Workshop on Kernel Machines. Heidelberg: Springer-Verlag*, 2003.

[3] P. Ren, R. C. Wilson, and E. R. Hancock, "Graph characterization via Ihara coefficients," *IEEE Tran. on Neural Networks*, vol. 22, pp. 233–245, 2011.

[4] B. Xiao, E. R. Hancock, and R. C. Wilson, "Geometric characterization and clustering of graphs using heat kernel embeddings," *Image Vision Comput.*, vol. 28, no. 6, pp. 1003–1021, 2010.

[5] B. Xiao, E. R. Hancock, and R. Wilson, "Graph characteristics from the heat kernel trace," *Pattern Recognition*, p. 25892606, 2009.

[6] J. Sun, M. Ovsjanikov, and L. Guibas, "A concise and provably informative multi-scale signature based on heat diffusion," *Comp. Grarph Forum*, pp. 1383–1392, 2010.

[7] U. Castellani, P. Mirtuono, V. Murino, M. Bellani, G. Rambaldelli, M. Tansella, and P. Brambilla, "A new shape diffusion descriptor for brain classification," *MICCAI*, pp. 426–433, 2011.

[8] M. Aubry, U. Schlickewei, and D. Cremers, "The wave kernel signature: A quantum mechanical approach to shape analysis," *Tech. rep., TU München, Germany*, 2011.

[9] P. Suau, E. R. Hancock, and F. Escolano, "Analysis of the schrödinger operator in the context of graph characterization," *Similarity based Pattern Recognition*, pp. 190–203, 2013.

[10] J. Friedman and J. P. Tillich, "Calculus on graphs," *CoRR*, 2004.

[11] R. C. Wilson, F. Aziz, and E. R. Hancock, "Eigenfunctions of the edge-based laplacian on a graph," *Linear Algebra and its Applications*, vol. 438, no. 11, pp. 4183–4189, 2013.

[12] H. ElGhawalby and E. R. Hancock, "Graph embedding using an edge-based wave kernel," *SSPR/SPR*, p. 6069, 2010.

[13] F. Aziz, R. C. Wilson, and E. R. Hancock, "Gaussian wave packet on a graph," *Graph-based representation*, 2013.

[14] F. Aziz, R. Wilson, and E. Hancock, "Analysis of wave packet signature of a graph," *15th International Conference on Computer Analysis of Images and Patterns*, 2013.

[15] F. Aziz, R. Wilson, and E. R. Hancock, "Shape signature using the edge-based laplacian," *International Conference on Pattern Recognition*, 2012.

[16] J. Friedman and J. P. Tillich, "Wave equations for graphs and the edge based laplacian," *Pacific Journal of Mathematics*, p. 229266, 2004.

[17] H. Murase and N. S. K, "Visual learning and recognition of 3-d objects from appearance," *International Journal of Computer Vision*, vol. 14, no. 1, pp. 5–24, 1995.

[18] C. Harris and M. Stephens, "A combined corner and edge detector," *In Fourth Alvey Vision Conference, Manchester, UK*, p. 147151, 1988.

[19] B. Delaunay, "Sur la sphre vide, izvestia akademii nauk sssr, otdelenie matematicheskikh i estestvennykh nauk," p. 793800, 1934.

[20] G. K. R and S. R. R, "A new statistical approach to geographic variation analysis," *Systematic Zoology*, p. 205222, 1969.

[21] G. T. Toussaint, "The relative neighbourhood graph of a finite planar set," *Pattern Recognition*, vol. 12, no. 4, pp. 261 – 268, 1980.

[22] I. T. Jolliffe, "Principal component analysis," *Springer-Verlag, New York*, 1986.

[23] S. Biasotti, S. Marini, M. Mortara, G. Patanè, M. Spagnuolo, and B. Falcidieno, "3d shape matching through topological structures," in *DGCI*, 2003, pp. 194–203.